Solid-State Electronics Vol. 23, pp. 1159–1169
Pergamon Press Ltd., 1980. Printed in Great Britain

ADMITTANCE SPECTROSCOPY: A POWERFUL CHARACTERIZATION TECHNIQUE FOR SEMICONDUCTOR CRYSTALS—APPLICATION TO ZnTe

J. L. PAUTRAT, B. KATIRCIOGLU, N. MAGNEA, D. BENSAHEL, J. C. PFISTER† and L. REVOIL
Centre d'Etudes Nucleaires de Grenoble Département de Recherche Fondamentale, Section de Physique du Solide, 85X 38041 Grenoble, Cédex, France

(*Received* 10 *December* 1979; *in revised form* 31 *January* 1980)

Abstract—The admittance spectroscopy technique is shown to be a very convenient tool for analyzing majority carrier traps: energy level, capture cross section and concentrations are easily obtained without complicated mathematical treatment. The series resistance in the material underlying the Schottky or pn junction is also detected when the free carriers are freezing out. It allows to get the shallowest level energy and its compensation ratio. The method has been applied to ZnTe material analysis and the effect on the admittance of six different acceptors is demonstrated. When comparing the electrically determined ionization energy of a given impurity with its optical value the former appears as systematically lower but most of the difference can be ascribed to Poole Frenkel or impurity concentration effects.

1. INTRODUCTION

The influence of deep levels on the impedance of a semiconductor device has been recognized for a long time[1–9] and this effect has been suggested as a way for deep trap analysis. The corresponding method has been described by Losee and called "admittance spectroscopy"[10]. Although the method has very appealing features its use has not been widely developed. The main works devoted to the analysis of a given material are those of Losee[10] (ZnTe and $Cd_{1-x}Zn_xTe$), Vincent *et al.*[11] (GaP), Desnica *et al.*[12] (GaP), Tokuda *et al.*[13] (irradiated Si), Brabant[14] (Si), and more recently Bensahel *et al.*[15](ZnTe), Kobayashi *et al.*[16] (CdS), and Hoffmann *et al.*[17] (GaAs).

By comparison the DLTS method[18] born at about the same time developed much more considerably. In conclusion of the paper we will compare both methods, the experimental equipment needed and the results they provide.

In the following we will give special attention to the theoretical and practical developments of the method which permitted us to use it as a very common tool for routine semiconductor characterization.

Furthermore all the experimental results have been compared with specific data drawn from photoluminescence analysis of the same samples, so that a very close correspondence between the nature of the impurities and the admittance features has been established. The comparison between the electrical and optical "signatures" of a given trap will be outlined and discussed.

In Section 2 the theoretical analysis of a semiconductor junction containing one deep trap is recalled. We establish the useful formula which give the emission parameters (energy level and capture cross section) and concentration of the deep center. The calculation is then extended to the case of more than one deep level.

The experimental details are presented in Section 3 and the analysis of the results is done in Section 4 for the shallowest level, in Section 5 for the deep ones. In Section 5.4 the case of a sample with three deep levels is more particularly detailed as an example of superposition of several deep levels.

2. THEORETICAL BACKGROUND

Among the various theoretical treatments of the impedance of a semiconductor junction the more complete one, is due to Beguwala and Crowell[9] allowing for an arbitrary number of deep species. An exact numerical solution due to Losee[10] needs a computer. In fact it is much simpler and generally sufficient to consider only one deep level. The extension to more complicated cases can be made easily if the response of the various deep levels does not occur in the same temperature or frequency range.

We suppose we are dealing with a Schottky diode made on a p-type material whose electric potential and field are represented on Fig. 1(a). Naturally all the analysis could be easily changed to describe n-type material. The deep level E_t crosses the Fermi level at point x_t while the shallower one E_s does not cross it. The concentrations are respectively N_t and N_s. If there is a compensating donor level one simply writes $N_s - N_d$ instead of N_s. The space charge extent is w.

2.1 *Deep level occupancy*

The detailed balance equations provide the basis for getting the level occupancy according to

$$\frac{dp_t}{dt} = c_p p(N_t - p_t) - e_p p_t \qquad (1)$$

where c_p and e_p are the capture and emission coefficients, p and p_t are the free and trapped hole densities. At equilibrium the level occupancy verifies the

†Université Scientifique et Médicale de Grenoble, France.

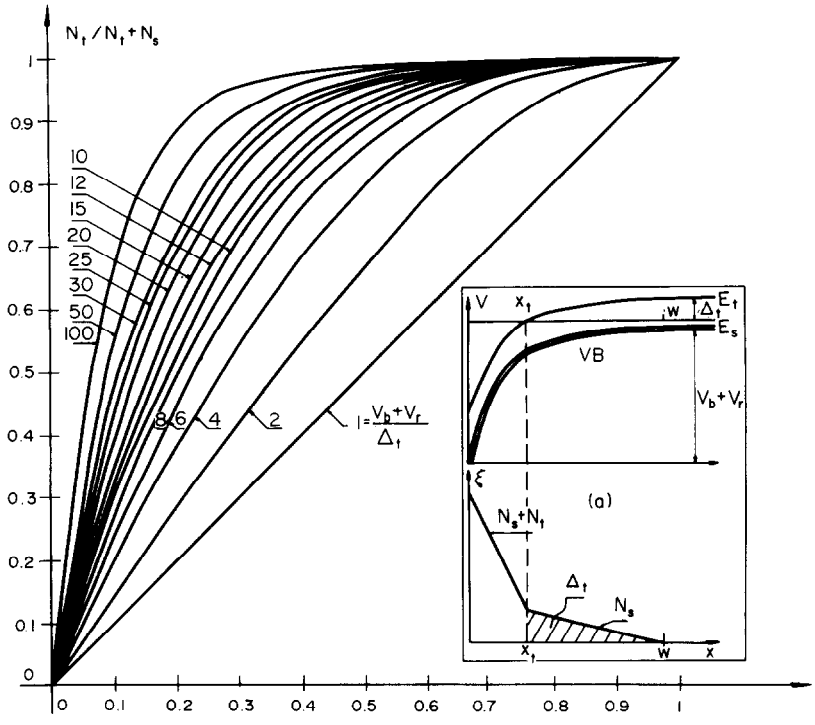

Fig. 1.

Fermi-Dirac distribution

$$p_t = N_t\left(1+g^{-1}e^{-\frac{E_t-E_F}{kT}}\right)^{-1} = N_t f_t \qquad (2)$$

if g is the level degeneracy factor, k the Boltzmann constant and T the temperature. From these equations one deduces the emission probability

$$e_p = c_p N_v g^{-1} e^{\frac{E_v-E_t}{kT}} \qquad (3)$$

where N_v is the valence band density of states.

Writing this expression we neglect all the exchanges with the conduction band. This is completely justified for a wide gap semiconductor since the levels considered are never more than ~0.5 eV away from the valence band. More complete equations should be used for materials where levels close to the midgap could be encountered[6].

Solving eqn (1) for p_t, in the case of a constant free hole density, yields an exponential relaxation characterized by a time constant

$$\tau^{-1} = e_p + c_p p = c_p(p+p_1) \qquad (4)$$

if

$$p_1 = N_v g^{-1} e^{\frac{E_v-E_t}{kT}}. \qquad (5)$$

In the space charge region p is not a constant and the deep level will be characterized by a distribution of time constants ranging from $c_p^{-1}(p_0+p_1)^{-1}$ in the bulk to $c_p^{-1}p_1^{-1}$ far from the edge (p_0 is the bulk free hole density).

2.2 *Trap response to an a.c. bias*

We suppose that the voltage drop across the space charge region is periodically modulated by a small a.c. voltage. The space charge extent w is also periodically modulated and, within a dielectric relaxation time, the free hole density and the hole quasi Fermi level at any point x of the space charge region are also modulated. Derivation of eqn (2) gives

$$\delta p_t = N_t \delta f_t = N_t f_t(1-f_t)(kT)^{-1}\delta v \qquad (6)$$

if δ refers to the a.c. quantities; δv being the a.c. bias. The fonction $f_t(1-f_t)$ is a peak of width ~4 kT centered around the point where $f_t = 1/2$. At this point;

$$E_t = E_F - kT\ln g \qquad (7)$$

In order to simplify this defines the point we call x_t and not, strictly speaking, the crossing point indicated on Fig. 1(a).

Combination of eqn (6) and (1) leads to a local differential equation which can be solved for $\delta p_t(x)$ and integrated in order to get the total a.c. charge on the deep states δQ_t [9, 14, 18]. However more convenient expressions are obtained if simplifying assumptions are made. One of these identifies the Fermi-Dirac distribution with a step like function[6]. Another hypothesis, somewhat

less restrictive, rests on the observation that according to eqn (6) the a.c. bias does not induce any appreciable modulation of the deep center occupancy outside a small region $\sim 4\,kT/q$ wide centered on x_t. Around this point $f_t(1-f_t)$ can be approximated by a triangularly shaped function of the same area. This hypothesis respects the true spreading of the a.c. charge and yields easily the total a.c. charge on the deep level. Doing this we only neglect the distribution of the time constants around its value at x_t which is;

$$\tau_0^{-1} = 2c_p p_1. \tag{8}$$

The final differential equation giving the a.c. charge is;

$$\frac{\mathrm{d}}{\mathrm{d}t}\delta Q_t = -\frac{\delta Q_t}{\tau} + \frac{\delta v}{R_t} \tag{9}$$

where

$$\tau^{-1} = \tau_0^{-1}\left[1 + \frac{x_t}{w}\frac{N_t}{N_s}\right] \tag{10}$$

and

$$R_t^{-1} = \tau_0^{-1}\frac{\epsilon}{w}\frac{N_t}{N_s}. \tag{11}$$

It is apparent from these equations that the characteristic time constant of the device is shifted with respect to that of the isolated deep center by a factor $(1 + x_t N_t/wN_s)$ arising from the coupling to the modulated free hole density.

2.3 *Admittance of the junction*

ω being the angular frequency of the a.c. bias a standard small signal treatment using eqn (9) leads to the admittance of the device[6];

$$Y = G + jC\omega \tag{12}$$

where

$$\frac{G}{\omega} = \Delta C\frac{\omega\tau}{1+\omega^2\tau^2} \tag{13}$$

with

$$\Delta C = \frac{\epsilon}{w}\frac{N_t}{N_s}\frac{1-\frac{x_t}{w}}{1+\frac{x_t}{w}\frac{N_t}{N_s}}. \tag{15}$$

C_{HF} and $C_{BF} = C_{HF} + \Delta C$ are respectively the high and low frequency limits of the capacitance. The real part G/ω has a peak of height $\Delta C/2$ at $\omega\tau = 1$.

2.4 *Determination of the concentrations of the deep and shallow centres*

The eqn (13)–(15) can be used to extract the concentration of the centres since x_t and w can be readily calculated using the Poisson equation and the depth of the trap.

Let us call

$$\Delta = (E_t + kT\ln g - E_F)q^{-1} \tag{16}$$

and V_b and V_r the built-in and externally applied voltages. We have

$$C_{HF}^{-1} = \frac{w}{\epsilon} = \frac{N_t}{N_t+N_s}\left(\frac{2\Delta}{q\epsilon N_s}\right)^{1/2} + C_{BF}^{-1} \tag{17}$$

$$C_{BF}^{-1} = \left(\frac{2}{q\epsilon(N_t+N_s)}\right)\left(V_b + V_r - \frac{N_t}{N_t+N_s}\Delta\right)\Big)^{1/2}. \tag{18}$$

The first interesting feature to point out is that the traditional $\mathrm{d}C_{BF}^{-2}/\mathrm{d}V$ plot has a slope related to the total density of impurities $N_t + N_s$ even if the deep one is not ionized in the bulk material. The voltage obtained by extraploating to $C_{BF}^{-2} = 0$ is now $V_b - \Delta N_t/(N_t + N_s)$ instead of V_b. With $\alpha = N_t/(N_t + N_s)$ and $A = \Delta C/C_{BF}$, the preceding equations lead to

$$A = 1 - [\alpha\sqrt{\Delta[(1-\alpha)(V_b + V_r - \alpha\Delta)]^{1/2} + 1}]^{-1} \tag{19}$$

which is a quadratic equation in α

$$\alpha^2\left[\frac{(A-1)^2}{A^2} - 1\right] + \alpha\left[\frac{V_b+V_r}{\Delta} + 1\right] - \frac{V_b+V_r}{\Delta} = 0 \tag{20}$$

whose positive solution is

$$\alpha = \frac{-\left[\frac{V_b+V_r}{\Delta}+1\right] + \left(\left(\frac{V_b+V_r}{\Delta}+1\right)^2 + 4\frac{V_b+V_r}{\Delta}\left(\frac{(A-1)^2}{A^2}-1\right)\right)^{1/2}}{2\left(\frac{(A-1)^2}{A^2}-1\right)}. \tag{21}$$

and

$$C = C_{HF} + \frac{\Delta C}{1+\omega^2\tau^2} \tag{14}$$

This function has been plotted in Fig. 1 for several values of $(V_b + V_r)/\Delta$. The resulting curves provide a very simple way of getting the relative concentration of the deep centers. A simplified expression of eqn (21) can

be obtained if the deep level concentration is low enough. In this case $A \ll 2\sqrt{(\Delta/V_b + V_r)}$ and then

$$\alpha = A\sqrt{\left(\frac{V_b + V_r}{\Delta}\right)}. \tag{22}$$

This expression illustrates the square root dependence of the capacitance step on the normalized depth of the level. The absolute values of concentrations are easily obtained since $N_t + N_s$ is given by the C_{BF}^{-2} vs V_r plot according to eqn (18) above.

The sensitivity of the method can be discussed on the basis of eqn (22). Let us suppose that there is a deep level at $E_v + 160$ meV and a shallow one whose density is about 10^{16} cm^{-3} so that the Fermi level is about at $E_v + 60$ meV. If $V_b = 0.9$ and $V_r = 0$ we get finally $\alpha = 3\Delta C/C$.

The smallest $\Delta C/C$ which can be detected is 1% but better resolution is achieved by looking at the real part of the admittance, whose peak height is $\Delta C/2$, since the useful signal is free from any background value. With commercially available apparatus, peaks corresponding to $\Delta C/C \approx 10^{-3}$ are easily detected so that the resolution is $N_t/N_s \approx 3 \times 10^{-3}$.

This does not represent the ultimate sensitivity of the method but rather the amount of deep impurities that should certainly be detected. This level of sensitivity is practically independent on the background doping level as long as the bulk conductivity is sufficient for the admittance to be measured. So if $N_s = 10^{14}$ cm^{-3}, with the same conditions as above $N_t \approx 3 \times 10^{11}$ cm^{-3}.

2.5 *Emission parameters*

The basic phenomenon is the time constant for capture and emission of carriers so that analysis of the characteristic time of the admittance spectrum leads to the intrinsic parameters of the trap.

This is apparent from eqn (13) which shows that the conductance is maximum when the condition $\omega\tau = 1$ is fulfilled. In fact eqn (13) and (14) result of the hypothesis made on the localisation of the a.c. charge around x_t. This hypothesis is not absolutely necessary and complete calculations have been done by Brabant[14], Vincent[18] which have shown that the conductance maximum is found for $\omega\tau = 1.98$ instead of $\omega\tau = 1$. It will be shown that this can induce the corresponding factor as an error on the capture cross section.

According to eqn (10) at the conductance maximum the following relation holds

$$1 = \omega\tau = \omega\tau_0\left[1 + \frac{x_t}{w}\frac{N_t}{N_s}\right]^{-1} \tag{23}$$

which can be expressed as

$$1 = \omega\tau_0 \frac{C_{BF}}{C_{HF}} \frac{N_s}{N_t + N_s} = \omega\tau_0 \frac{1-\alpha}{1-A} \tag{24}$$

where A and α are the quantities defined above. τ_0 can be expressed with eqns (5) and (8) so that the preceding equation can be written as

$$\omega = \frac{1-A}{1-\alpha} 2c_p g^{-1} N_v \exp(E_t + kT \ln g - E_v)/kT. \tag{25}$$

The conductance peak is obtained either at a fixed temperature varying the frequency, or at a fixed frequency varying the temperature. This last method is more generally used since the experimental set up is simpler. In both cases a set of (T, ω) values are obtained. In order to extract the emission parameters all the temperature dependent terms have to be explicited. First, as usually, the capture probability c_p can be expressed as an effective cross section σ_p times the thermal velocity of carriers ($1/2m_p^* v_t^2 = kT$; m_p^* being the effective mass of the holes). The density of states can be written as $N_v = Bm_p^{*3/2}T^{3/2}$ where B is a constant independent of temperature.

Finally eqn (25) can be put in the form.

$$\omega T^{-2} = \left[\frac{1-A}{1-\alpha} 2\sqrt{(2k)}Bm_p^*\right]\sigma_p \exp(E_t - E_v)/kT \tag{26}$$

since terms containing g cancel.

If the temperature dependence of σ_p can be neglected, the plot of $\mathrm{Ln}\,\omega T^{-2}$ vs T^{-1} gives a straight line whose slope is $(E_t - E_v)/k$ and whose intercept with the ω axis is related to σ_p since the bracketted factor is easily calculated from the experimental data.

It is particularly important to note that the activation energy is related to the effective depth of the level around x_t. We have shown recently that this value can differ significantly from the true depth of the level due to the electric field around x_t and to the interaction between close impurities which induce a significant lowering of the coulombic barrier around the impurity[19]. The corresponding correction can be calculated and so the "zero field, low concentration" depth of the level can be obtained. This value can eventually be compared with an optically determined ionization energy and both should be identical if there are no complications like that arising from a Franck–Condon shift.

2.6 *Summary of the analysis of the experimental data*

Let us suppose we have a device containing only one deep level. The overall doping $N_s + N_t$ is deduced from a C_{BF}^{-2} vs V_r plot at say 300 K. The device is characterized by a set of G/ω vs T curves at several frequencies which yield a set of peak temperatures and a frequency independent peak height. (a) The plot of ωT^{-2} vs T^{-1} gives $E_t - E_v$ (eqn 26) (b) A supposed value is taken for N_s in order to calculate the Fermi level position and $\Delta = E_t - E_F + kT \ln g$. (c) The relative deep level concentration is then obtained from eqn (21) or from the curves given in Fig. 1 using the peak height. A self consistent calculation is made by correcting the N_s value in step (b). (d) The capture cross section is obtained from the plot made in (a), using the result of calculation made in (c) for establishing the correcting factor of eqn (26).

2.7 *More than one deep level*

The general problem of many defect levels and of their effects on the admittance has very complicated solutions[9]. We want to show that for practical problems most of the interesting data can be obtained using the one-level calculations given above. Let us suppose there is a second level at an intermediate depth E_m between E_t and the shallow level. This level crosses the Fermi level at x_m and its occupancy is governed by an equation similar to eqn (9) but equations related to the different levels are now coupled via the free hole density so that the characteristic time constants will be shifted again from their intrinsic values. The complete solutions have been already obtained[6], and they show that the coupling may increase the separation between close peaks. But, in fact, this coupling will be important only for levels which are so close that their relaxation occurs in the same range of temperature and frequency. This concerns levels which are closer than kT if they have about the same σ_p. Such levels will frequently appear as a single level since all the energies are distributed around a mean value due to the lowering factors outlined above. This means that the coupling may contribute to the widening of the response due to a band of closely distributed levels. Nevertheless the shift of the response due to the coupling between the levels will only affect the capture cross section and not the activation energy.

Let us go now to the case of well separated deep levels. Their responses appear as individual peaks in the conductance curve. Fron an a.c. point of view they can be treated separately but, nevertheless, all the levels contribute simultaneously to the space charge and so the levels can be considered as d.c. coupled. We will show that quite simple arguments allow to extend the single level treatment to the present case.

The situation is shown is Fig. 2. The index m is used for the intermediate level. As in the single level case, the high temperature capacitance voltage curve yields $N_s + N_m + N_t = N$.

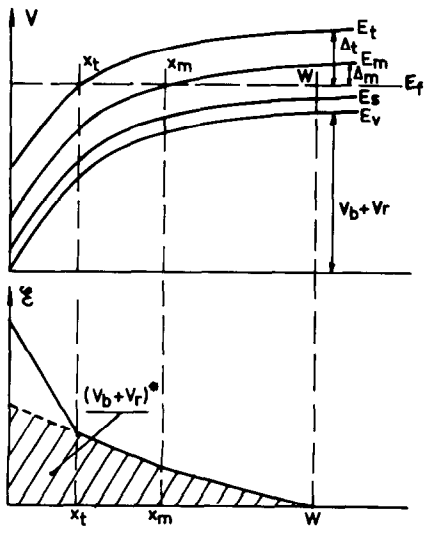

Fig. 2. Diagram of the potential and electric field within a Schottky diode containing two deep levels at E_t and E_m. Their respective depths above the Fermi level are Δ_t and Δ_m. The shaded area shows the effective voltage $(V_b + V_r)^*$ used for calculating the concentration of the intermediate level at E_m.

Lowering the temperature freezes out the a.c. response of the deepest level E_t and the concentrations of this level can be calculated ignoring the E_m level inasmuch as this level may well be yet under the Fermi level so that x_m and w are either confused or very close to each other.

Going to lower temperatures, the Fermi level crosses the level E_m. This can be accompanied by a very small change of capacitance known as the capacitance edge effect[20] not accompanied with any conductance term and generally not seen as a very characterized feature. But x_m and w become progressively well separated and at a given temperature the level E_m, itself, is frozen out. The displacement of the conductance peak with frequency can be used to get the depth of the level whereas its concentration cannot be obtained so directly since the deepest level is always acting on the space charge configuration. In fact a very simple way of ignoring this level, keeping the same values of x_m and w is to reduce $V_b + V_r$ to some effective value; $(V_b + V_r)^*$. The situation is shown in Fig. 2 where this effective value is represented by the shaded area. The one level calculation can now be used again without any restriction starting from the $\Delta C/C$ obtained for level m. This method can be repeated successively for any number of levels, without any restriction on the density of the various species.

The calculation of the effective voltage $(V_b + V_r)^*$ is given in the appendix.

3. EXPERIMENTAL RESULTS

The results presented here to illustrate the method have been obtained on ZnTe, a p-type II VI compound which is becoming a very well known semi-conductor. Admittance spectroscopy has been one of the useful tools which, combined with high resolution luminescence spectroscopy and scanning electron microscopy, allowed us to progress in the understanding of this material. Particularly the admittance spectroscopy results will be compared as often as possible with the luminescence data which provide a unique tool for identification of the impurities[21–23].

3.1 *Preparation of the samples and experimental techniques*

The ZnTe crystals are grown from a Te-rich melt at about 1100°C. After sawing the slices are mechanically and chemically polished. If back doping is wanted a metallic layer of the dopant (e.g. Cu, Ag, Au, etc.) is evaporated on the slice which is then annealed at a temperature depending on the particular impurity involved (generally between 300 and 500°C) in a N_2–H_2 gas mixture. After this treatment the metallic layer is etched-off and, generally the sample is mechanically bevelled to provide in depth analysis of the impurity content. After that a final chemical etching is done.

Schottky diodes are obtained by evaporating indium through a metallic mask ($\phi = 0.4$ mm). The ohmic contact is obtained by electroless gold plating on the back sur-

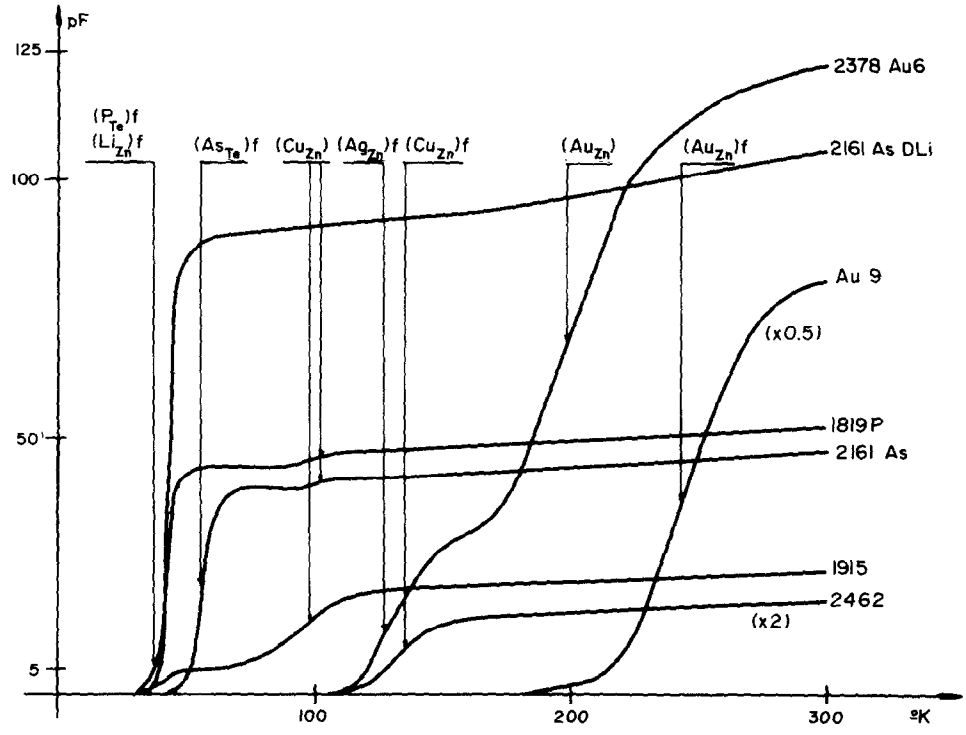

Fig. 3. Capacitance vs temperature curves obtained for Schottky diodes made on various ZnTe crystals whose characteristics are described in Table 1. The labels indicate the impurity responsible for each step. The subscript f is used for labelling the hole freezing-out steps.

face. The sample is mounted on a transistor header and a gold wire is bonded to the indium electrode.

For variable temperature measurements the sample is fitted into a variable temperature cryostat. The temperature is measured by a thermocouple fixed as close as possible to the sample. In non steady state conditions there is a small temperature difference (0.15 K) between the thermocouple and the sample as evidenced by the "hysteresis" obtained on successive heating and cooling operations. The central value is taken as the exact temperature.

Electrical measurements have been done with several apparatus; analog capacitance meter, automatic capacitance bridge, double phase lock-in amplifier. The results are identical if the a.c. voltage on the diode is kept as low as possible (~50 mV rms). Naturally the final accuracy of the activation energies depends on the accessible range of frequencies which cover at least one decade.

3.2 *Survey of the general properties of some samples*

On Fig. 3 we have gathered the $C(T)$ curves obtained for several typical samples whose particular doping or thermal treatments are indicated in Table 1.

Analysing such curves it is first important to note that the lowest temperature step of each curve (labelled with the subscript f) denotes simply the onset of a series resistance incompatible with the measurement at frequency f of the Schottky diode capacitance. This is the resistance of the bulk material underlying the diode whose value increases rapidly when the holes are being frozen out. The data that can be extracted from this part of the curves are discussed in the next section.

Now all the other steps in the curves of Fig. 3 have to be attributed to levels deeper than the shallowest uncompensated acceptor involved in the hole freezing-out. It is clear that a given impurity may be either in the situation of a deep level (for instance Cu in sample 1819) or in the situation of shallowest level (Cu in sample 2462 or Au 6). Both kinds of steps do not coincide exactly due to differences in preexponential factors of both phenomena. All the data that can be deduced of the deep level steps are analysed in Section 5.

In fact the precise attribution of all the steps rests on a close comparison of the electrical data shown here with photoluminescence data which allow unambiguous identification of most of the impurities contained in a given sample.

4. FREEZING-OUT OF THE FREE CARRIERS

As the free carrier density decreases, the resistance R_s in series with the device of capacitance C becomes significant. The measured admittance results from the series to parallel conversion of the R_s, C network. The straightforward result is that the measured capacitance is $C/2$ when $\omega R_s C = 1$.

The spreading resistance expresses simply as

$$R_s = \rho/4r. \tag{27}$$

Where ρ is the resistivity of the material and r the radius of the electrode.

$$\rho^{-1} = pq\mu_p \tag{28}$$

Table 1. Electrical characteristics of the samples whose hole freezing out is shown in Fig. 3. N_s is the concentration of the shallowest acceptor and N_d the concentration of the compensating donors

Sample	Treatment	Shallowest acceptor / ionization energy in meV	Freezing activation energy meV	$N_s - N_d$ cm^{-3}	N_d cm^{-3}
1915	no	Li/61	-	$1.4\ 10^{14}$	$6.7\ 10^{12}$
D Li	Li diffused at 550°C	Li/61	56,5	3.10^{16}	$2.7\ 10^{14}$
1819	P doped at growth	P/ 63.5	59	$2.77\ 10^{16}$	$0.92\ 10^{14}$
2161	As doped at growth	As/75	73	$1.36\ 10^{16}$	$2.52\ 10^{14}$
DAu 6	Gold diffused at 550°C	Cu /149+Ag/123	124	$2.2\ 10^{15}$	$1.78\ 10^{14}$
2162	no	Cu/149	140	$1.4\ 10^{15}$	$2.9\ 10^{14}$
2462	no	Cu/149	145	$5\ 10^{14}$	$1.6\ 10^{14}$
DAu 9	Gold diffused at 650°C	Au/272	270	$1.6\ 10^{17}$	$9.3\ 10^{14}$

where p is the free hole density and μ_p is the mobility of the carriers. Thus in the middle of the step

$$\omega = 4rq\mu_p p/C. \tag{29}$$

If the carrier mobility is known this provides a simple method for evaluating the free carrier density vs temperature, like in a conventional R_s vs T measurement. This method is particularly attractive since there is no need for good non rectifying ohmic contacts. Naturally we do not know the exact mobility of the carriers, however, in ZnTe the carrier relaxation is essentially dominated by the lattice scattering, the temperature dependence of which can be well approximated by the law $\mu_h = \mu_0 T^{-2.5}$ in the range 60–300 K [24, 25] for doping in the range of 10^{15} cm^{-3}. With this approximated mobility law, and using

$$p = Bm_p^{*3/2} T^{3/2} \exp -(E_F - E_v)/kT$$

we get

$$\omega T = [4rq\mu_0 B m_p{}^{*3/2} C^{-1}] \exp -(E_F - E_v)/kT. \tag{30}$$

A plot of log ωT vs T^{-1} gives a straight line whose slope is $(E_F - E_v)$ extrapolated to $T = 0$. It is known that this extrapolation gives $E_A/2$ if the crystal is absolutely non compensated and E_A if there is a small compensation, which is the general situation.

The curves displayed on Fig. 3 show that the freezing temperatures vary considerably from sample to sample and the activation energies of the linear plots obtained in Fig. 4 vary in the same way. The values obtained are very close to the optically determined ionization energy of the shallowest uncompensated acceptor. The nature of this acceptor has been obtained from the treatment to which the sample was submitted and from the optical detection of the acceptor present. The supplementary information given by the present measurements is the concentration of the various levels and the indication of the Fermi level position. For example, in the case of sample *D* Au9, the level associated with Cu_{Zn} (149 meV), which was present in the starting material [21] has become completely compensated after the gold diffusion as evidenced by the Fermi level pinning at 270 meV. On the other hand a milder gold diffusion is always accompanied with the appearance of a small quantity of silver, like in DAU 6 (see also Section 5.4) which induces the Fermi level pinning near 123 meV. This is, in fact, a secondary effect of the diffusion experiment since silver release on annealing has been previously observed in ZnTe [15].

These results show that the series resistance can well be used for identifying the shallowest uncompensated level at least in II–VI compounds where impurity effects on the mobility are small.

Another important value that can be deduced from these hole freezing experiments is the compensation ratio. Since the $C(T)$ curve can be transformed in a $p(T)$ curve, we can obtain the Fermi level position and thus deduce the amount of compensating centres. A detailed

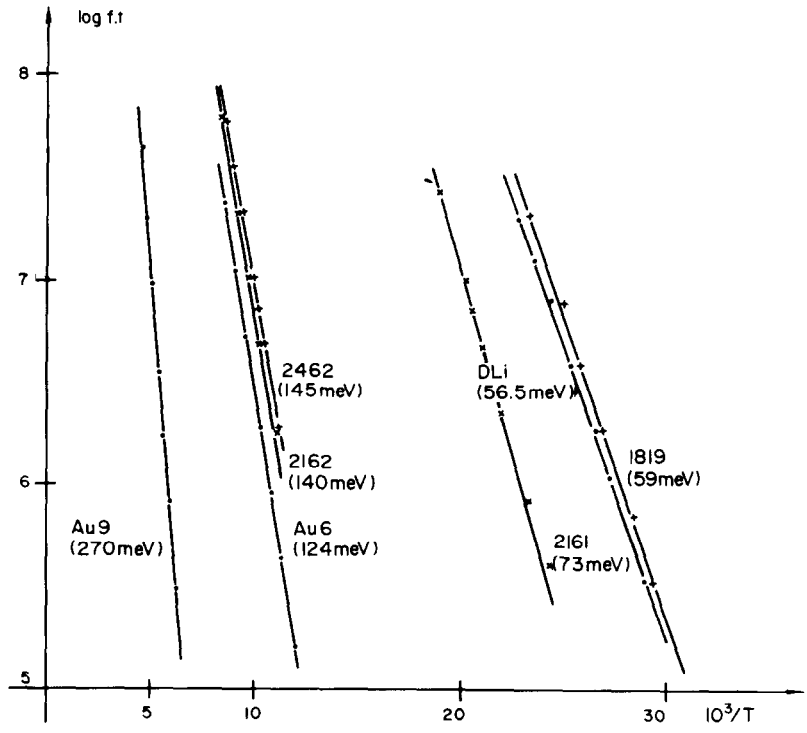

Fig. 4. Plot of $\ln fT$ vs T^{-1} for the hole freezing steps.

account of this method is being prepared for publication[26] but the corresponding results have been reported here in Table 1.

5. DEEP LEVEL ANALYSIS

As noted in Section 2.6. a complete set of $C(T)$ or $G(T)$ curves at various frequencies allows to determine all the parameters of a given deep level.

5.1 *Energy level*

It is deduced from the plot of $\log \omega T^{-2}$ vs T^{-1} where T is the conductance peak obtained at frequency ω. The results concerning the centers Au_{Zn} and Cu_{Zn} are plotted on Fig. 5 for samples whose characteristics are summarized in Tables 2 and 3.

The lines obtained show activation energies ranging between 210 and 244 meV for Au_{Zn} and between 94 and

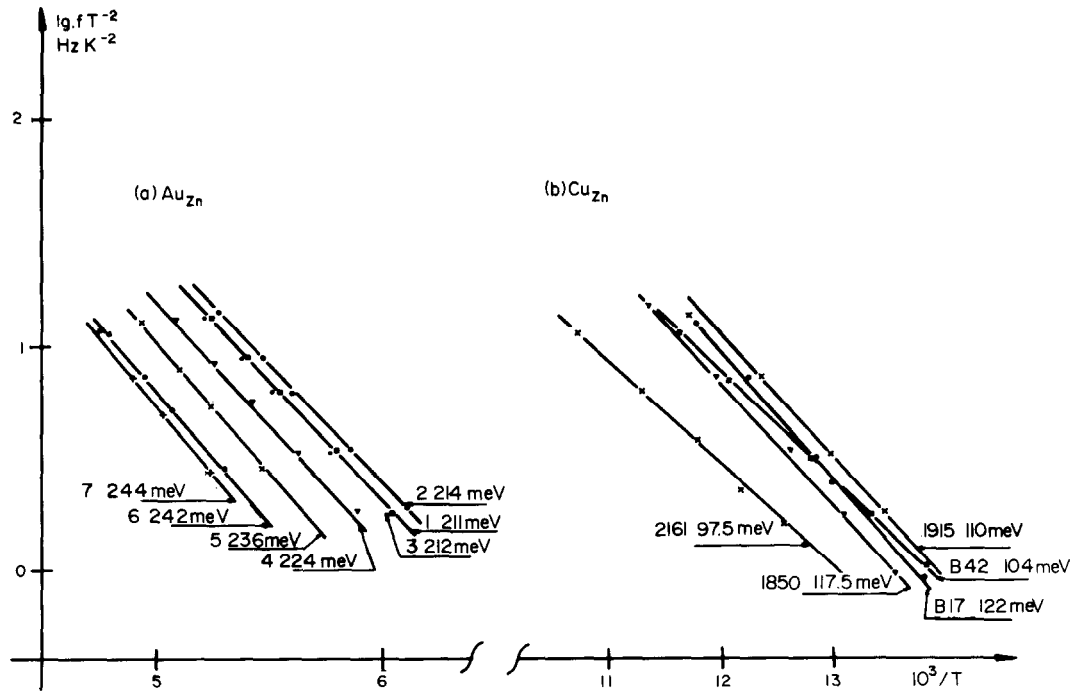

Fig. 5. Plot of $\ln fT^{-2}$ vs T^{-1} for the deep level steps associated with two impurities; (a) Au_{Zn}; (b) Cu_{Zn}.

Table 2. Electrical parameters of several Schottky diodes obtained on a gold diffused sample. $\Delta C/C$ is the relative height of the gold associated capacitance step. N_t and N_s are respectively the concentrations of the deep (gold) and shallow (copper, silver and phosphorus) acceptors. E_a is the experimental activation energy. ΔE is the theoretical lowering and E_{corr} is the corrected value ($E_a + \Delta E$). E_A^{Au} is the optically measured ionization energy of Au_{Zn}. σ is the corrected capture cross section

Sample	$\Delta C/C$	N_t x 10^{15} cm^{-2}	N_s x $10^{15} cm^{-2}$	E_a meV	ΔE meV	E_{corr} meV	E_A^{Au} meV	σ 10^{-15} cm^{+2}
Au 1	.468	39.8	6.2	211	38.6	249.6	272,0±1	3.38
Au 2	.523	46.9	4.7	214	33.9	247.9	"	2.46
Au 3	.5	27.0	3.0	212	32	244	"	1.9
Au 4	.42	13.3	2.7	224	31.9	255.9	"	4.23
Au 5	.33	5.2	1.7	236	29.6	265.6	"	12.1
Au 6	.262	2.7	1.7	242	29.2	271.2	"	11.5
Au 7	.238	2.3	1.7	244	29.7	273.7	"	10.3

Table 3. Electrical parameters related to the Cu_{Zn} centers obtained from Schottky diodes made on several crystals (see Table 1 for details on the crystal treatments). The columns are labelled as in Table 2

Sample	$\Delta C/C$	N_t x $10^{15} cm^{-2}$	N_s x $10^{15} cm^{-2}$	E_a meV	ΔE meV	E_{corr} meV	E_A^{Cu} meV	σ $10^{-14} cm^2$
B 17	0.222	30.3	37.9	122	47.5	169.5	149	140
B 42	0.33	6.25	1.24	104	22.5	126.5	"	1.97
2161	0.027	1.44	12.5	97.5	38.9	136.4	"	1.12
1850	0.516	5.72	2.78	117.5	14.6	132.1	"	2.28
1915	0.713	5.46	.03	110	19	129	"	0.36

117.5 meV for Cu_{Zn}, so that the attribution to one center of each group of lines may seem quite unreasonable. However, in each case the high resolution photoluminescence spectra of these samples display the lines associated with the well defined acceptor levels respectively at 272 and 149 meV. Furthermore we have remarked that the high doping levels are always associated with the lower activation energies. This led us to investigate the electric field and impurity concentration effects on the ionization energy of the impurities[19]. The electric field in the space charge region near the point x_t produces a Poole-Frenkel lowering of the Coulombic barrier. Similarly the random electric field due to nearby ionized impurities reinforces the lowering. Combination of both effects has been calculated and the correction is displayed as ΔE in Tables 2 and 3. The corrected values are now all around the optical values except in the case of highly concentrated gold samples for which the corrected values remain about 10% too low. This point is discussed in Ref. [19].

This proves that admittance spectroscopy can be a good method for the evaluation of the ionization energies. The accuracy is about 4% but the various barrier lowering phonomena have to be corrected for. Such lowerings are expected to affect DLTS or TSCAP results to a similar or greater extent[19]. This means that the electrical "signature", defined as the emission rate vs temperature, taken as a characteristic feature of a given center[27] is in fact a relatively elusive notion depending greatly on environmental factors. When available the optical signatures like that arising from the two hole or two electron transitions appear to be much more reliable[22].

5.2 *Capture cross section*

From the same Fig. 5, extrapolation to infinite temperature yields a capture cross section using eqn (25). The correcting factor $(1 - A)/(1 - \alpha)$ is computed for each case, with an additional factor $kT/\Delta E$ introduced by the three dimensional Poole-Frenkel analysis[19] and the final values are listed in Tables 2 and 3. The dispersion is essentially due to the activation energy measurement. These results provide a useful order of magnitude but they cannot replace a direct measurement of the capture cross section and of its temperature dependence.

5.3 *Concentration*

The unique information that is brought out by the admittance measurements is the concentration of the deep levels. This is done simply using eqns (21) and (22) or the plot of Fig. 1. The quantity $\Delta_t = E_t - E_F + kT \ln g$ is easily calculated as indicated above using a trial value for N_s. The concentrations reported in Tables 2 and 3 have been computed according to this procedure. The

validity of the method can be checked in the following way. Several $C(T)$ curves of the sample Au 6 have been drawn for different values of the reverse bias and they have been independently used for the deep level analysis with the same built in voltage and total concentration. The dispersion (about 2% on $N_t/N_t + N_s$) seems to be due only to the uncertainties on ΔC (see Table 4). Additional systematic errors can be ascribed to the imprecision on Δ_t. Since the activation energy is known to about 5%, this leads to about a similar error of 5% on $N_t/N_t + N_s$ in the case of sample Au6.

5.4 *Superposition of several deep levels*

This is a frequently encountered situation and the main questions to solve are related to the energy separation between close levels and to the independent determination of each concentration. A typical situation is obtained in ZnTe when the acceptors Ag_{Zn} (123 meV) and Cu_{Zn} (149 meV) are simultaneously present. This is the case of the $C(T)$ and $\theta(T)$ curves represented in Fig. 6

Table 4. Concentration of the deep Au_{Zn} level deduced from several $C(T)$ curves drawn with various reverse biases for sample Au 6. The same $V_b = 0.9\ V$ and $N_t + N_s = 1.410^{17}\ cm^{-3}$ have been used

V_r volts	0	0.5	1	1.5	2
$\Delta C/C$	0.627	0.575	0.52	0.483	0.452
N_t $10^{17}\ cm^{-3}$	1.326	1.330	1.322	1.317	1.313
N_s $10^{15}\ cm^{-3}$	7.4	6.97	7.8	8.23	8.65

obtained after a gold diffusion in a crystal containing a small amount of phosphorus introduced at growth. Gold is the main acceptor ($N_t = 4.64 \times 10^{16}\ cm^{-3}$) and the phosphorus doping ($N_s = 3.32 \times 10^{15}\ cm^{-3}$) insures bulk conductivity until very low temperatures but optical measurements reveal the existence of the Cu_{Zn} and Ag_{Zn} impurities. The corresponding steps are hardly distinguished on the capacitance curve but very well separated in the phase angle. The frequency variations yield activation energies of 83 and 109 meV whose difference reflects exactly the distance between levels (26 meV). Both values have to be corrected by about 25 meV to account for the various lowering effects, but the final values (108 and 134 meV) remain about 10% too low. This last difference can be ascribed to the temperature dependence of the capture cross section[19].

The concentrations of these impurities are approximately identical and they are determined according to the method developed in Section 2.7. The result is $[Cu_{Zn}] = 9.33 \times 10^{14}\ cm^{-3}$ and $[Ag_{Zn}] = 8.87 \times 10^{14}\ cm^{-3}$.

6. CONCLUSION

The admittance spectroscopy method is a very powerful method whose usefulness has been proved with experimental results obtained on ZnTe.

We have shown that capacitance or conductance vs temperature curves on a large frequency range allow to determine the concentration, activation energy and capture cross section of one or several deep levels. The same measurements display the spreading resistance variation with temperature in the hole freezing region which allow to identify the shallowest levels and give its compensation ratio.

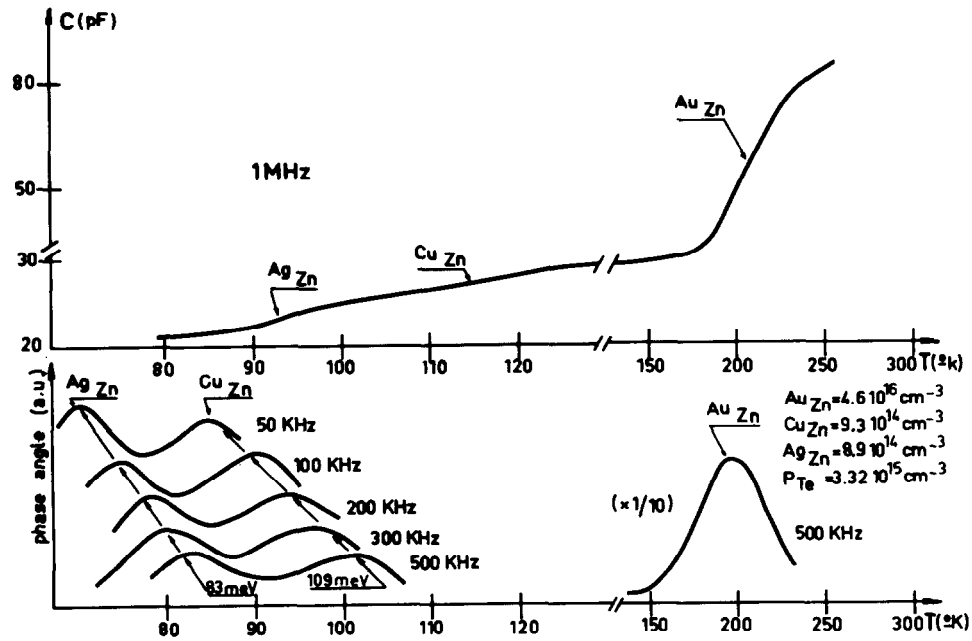

Fig. 6. Capacitance-temperature and phase angle-temperature curves obtained for a Schottky diode made on a crystal containing three deep levels Au_{Zn}, Cu_{Zn} and Ag_{Zn}. The background doping is due to P_{Te}. The concentration of the various impurities is indicated.

All those data are obtained on a very localized area defined by the Schottky diode or p–n junction area. This method is particularly convenient for experiments involving localized treatments like ion implantation, shallow perturbation due to annealing etc. Routine controls are easily performed with a standard fixed frequency capacitance meter and a variable temperature system and unless the mobility value is explicitly needed the admittance spectroscopy method seems to be much more useful for semiconductor samples analysis than the classical Hall-resistivity method. There is no need for efficient ohmic contact, specially shaped sample, magnetic field etc.

If the comparison with the very well known DLTS method has to be done one can outline that both methods are basically the same. The admittance method uses harmonic analysis and the DLTS technique used step response of the device. The electronic equipment needed is certainly less sophisticated in the harmonic method, while the sensitivity may be a bit lower since the deep level response is furnished only by a small region, $\sim kT$ wide, around x_t and not by the whole space charge region as in the standard DLTS technique.

On the other hand electric field effects on the ionization energy are more easily controlled with the admittance method. The major difference is that DLTS experiments made on p–n junctions can yield both electron and hole traps in the same substrate material whereas the admittance method will always detect only the majority carrier traps.

The present work based on a close comparison of optical and electrical data on ZnTe shows that in this material there is practically no discrepancy between both sets of data. Namely the Frank Condon shift, if any, is less than kT and well within the experimental uncertainty even for the deepest level analyzed, which is about at 4.5 times the hydrogenic level.

REFERENCES

1. C. T. Sah and V. G. K. Reddi, *IEEE Trans. Electron Dev.* **ED12**, 345 (1964).
2. E. Schibli and A. G. Milnes, *Solid-St. Electron.* **11**, 323 (1968).
3. V. I. Perel and A. L. Efros, *Sov. Phys. Semicond.* **1**, 1403 (1968).
4. G. I. Roberts and C. R. Crowell, *J. Appl. Phys.* **41**, 1767 (1970).
5. W. Schultz, *Solid-St. Electron.* **14**, 227 (1971).
6. W. G. Oldham and S. S. Naik, *Solid-St. Electron.* **15**, 1085 (1972).
7. Y. Zohta and Y. Ohmura, *Appl. Phys. Lett.* **21**, 117 (1972).
8. G. I. Roberts and C. R. Crowell, *Solid-St. Electron.* **16**, 29 (1973).
9. M. Beguwala and C. R. Crowell, *Solid-St. Electron.* **17**, 203 (1974).
10. D. L. Losee, *Appl. Phys. Lett.* **21**, 54 (1972); D. L. Losee, *J. Appl. Phys.* **46**, 2204 (1975).
11. G. Vincent, D. Bois and P. Pinard, *J. Appl. Phys.* **46**, 5173 (1975).
12. U. V. Desnica, B. Etlinger and N. B. Urli, *Int. Conf. on Radiation Effects in Semiconductors*, p. 402. The Inst. of Physics, London (1976).
13. Y. Tokuda and A. Usami, *J. Appl. Phys.* **48**, 1668 (1977).
14. J. C. Brabant, Thèse, Toulouse, France (1977) (unpublished).
15. D. Bensahel, N. Magnea, J. L. Pautrat, J. C. Pfister and L. Revoil, *Inst. Phys. Conf. Ser.* No. 46 p. 421, London (1979).
16. A. Kobayashi and T. Mori, *Appl. Phys.* **18**, 345 (1979).
17. H. J. Hoffman and H. Reisser, *Phys. Stat. Sol.* (a)**51**, K171 (1979).
18. G. Vincent, Thesis Lyon, France (1978) (unpublished).
19. J. L. Pautrat, *Solid-St. Electron.* **23**, 6 (1980).
20. C. T. Sah and J. W. Walker, *Appl. Phys. Lett.* **22**, 384 (1973).
21. N. Magnea, D. Bensahel, J. L. Pautrat and J. C. Pfister, *Phys. Stat. Sol.* (b)**94**, 627 (1979).
22. P. J. Dean, H. Venghaus, J. C. Pfister, B. Schaub and J. Marine, *J. Lum.* **16**, 363 (1978).
23. N. Magnea, D. Bensahel, J. L. Pautrat, K. Saminadayar and J. C. Pfister, *Solid-St. Comm.* **30**, 259 (1979).
24. M. Aven, *J. Appl. Phys.* **38**, 4421 (1967).
25. T. L. Larsen, Thesis, Stanford U.S.A. (1970).
26. J. L. Pautrat, (To be published).
27. A. Mircea and D. Bois, *Inst. Phys. Conf. Ser.* No. 46, p.83, London (1979).

APPENDIX

The problem is to get $(V_b + V_r)^*$ represented by the shaded area in Fig. 2 starting from $(V_b + V_r)$, total area under the electric field curve. The voltage drops between w and x_m on one hand and w and x_t on the other are called Δ_m and Δ_t respectively.

$$V_b + V_r = \frac{1}{2\epsilon}[N_s w^2 + N_m x_m^2 + N_t x_t^2] \tag{A1}$$

and

$$(V_b + V_r)^* = \frac{1}{2\epsilon}[N_s w^2 + N_m x_m^2]. \tag{A2}$$

$N = N_t + N_s + N_m$ and N_t are supposed to be known from the standard 1-level calculation (see Section 2.4). One needs only x_t to get the corrected $(V_b + V_r)^*$. It is more easily derived using another form of eqn (A1)

$$V_b + V_r = \Delta_t + x_t E_t + \frac{1}{2\epsilon} N x_t^2 \tag{A3}$$

where E_t is the electric field at point x_t, which is easily calculated as

$$E_t = \left[\frac{2(N_s + N_m)}{\epsilon}\left(\frac{N_s}{N_s + N_m}\Delta_m + \Delta_t - \Delta_m\right)\right]^{1/2} \tag{A4}$$

From eqns (A3) and (A4) we can get explicitly x_t and finally

$$(V_b + V_r)^* = (V_b + V_r) - \alpha_t(1 - \alpha_t)\Delta \times\left[-1 + \sqrt{\left(1 + \frac{V_b + V_r - \Delta_t}{(1 - \alpha_t)\Delta}\right)}\right]^2 \tag{A5}$$

where

$$\alpha_t = N_t/N$$

and

$$\Delta = \frac{N_s}{N_s + N_m}\Delta_m + \Delta_t - \Delta_m.$$

$\Delta_t - \Delta_m$ is simply the difference between the activation energies of conductance peaks related to both levels. Δ_m can be obtained from the activation energy and from the knowledge of the Fermi level at the relaxation temperature. This needs N_s but $N_s/N_s + N_m$ is the final result of the calculation using the corrected value $(V_b + V_r)^*$. So a self consistent calculation is needed if precise values are sought.